JOURNAL OF APPLIED ELECTROCHEMISTRY 9 (1979) 321–327

Electrochemical and chemical reactions involving non-equilibrium species at the nickel hydroxide electrode

R. S. SCHREBLER GUZMÁN, J. R. VILCHE, A. J. ARVÍA

Instituto de Investigaciones Fisicoquímicas Teóricas y Aplicadas (INIFTA), División Electroquímica, Sucursal 4, Casilla de Correo 16, 1900 La Plata, Argentina

Received 28 April 1978

The square-type reaction scheme proposed to interpret the behaviour of the nickel hydroxide electrode in KOH solutions under non-equilibrium conditions must include electrochemical as well as chemical crossed reactions between the different transient species. These reactions are evidenced by means of the triangularly-modulated triangular potential sweep technique. The contribution of the crossed reactions in the square-type reaction scheme becomes more relevant as the KOH concentrations decreased in the presence of K_2SO_4 supporting electrolyte.

1. Introduction

Under dynamic potential perturbations the nickel hydroxide electrode exhibits a relatively complex kinetic response due to the non-equilibrium states of both reactants and products. Thus, under properly adjusted conventional triangular potential sweeps at least two reduced and two oxidized states are clearly detected and the chemical transformations among the corresponding reactants and products have been demonstrated [1–3]. The simplest representation of those electrochemical and chemical processes related to the nickel hydroxide electrode has been given in terms of a square reaction scheme such as:

$$\begin{array}{ccc} \alpha\text{-Ni(OH)}_2 & \rightleftharpoons & \gamma\text{-NiOOH} + H^+ + e \\ \uparrow\downarrow & & \uparrow\downarrow \\ \beta\text{-Ni(OH)}_2 & \rightleftharpoons & \gamma\text{-NiOOH} + H^+ + e \end{array} \quad (1)$$

where the different substances were tentatively identified in terms of the different species structurally distinguished by other authors [4–6]. The proposed reaction scheme, however, leaves open the possibility of a contribution from the crossed processes which remain unnoticed, at least with the perturbation technique then used.

In an attempt to obtain a more detailed knowledge of these reactions, various Ni–alkaline solution interfaces were studied under triangularly-modulated single triangular potential sweep perturbations, a technique introduced a few years ago to investigate the electrosorption and electrodesorption of hydrogen adatoms on platinum [7] and, more recently, of oxygen on various metals under different conditions [8, 9].

The triangularly-modulated either linear or triangular potential sweep is usually a convenient technique to detect electrochemically produced intermediate species of relatively short lifetimes. It consists essentially of either a linear or a triangular potential sweep at a low rate (base signal) and a superimposed triangular potential modulation at a fast rate (modulating signal) and of smaller amplitude. The fast triangular potential sweep makes, in principle, a progressive sampling and analysis of the reactants and products which are involved in the electrochemical reactions within a small potential range as the guide ramp advances in either direction [7]. The overall potential/current response depends on both the guide ramp sweep rate to the modulating signal sweep rate ratio and the amplitude of the modulating signal [8].

The overall electrochemical response of the Ni/alkaline solutions interfaces confirms the previous findings [1–3] and shows, under a certain range of perturbation conditions, the existence of the

crossed reactions; their contribution to the overall process depends on the time scale involved in the relaxation process and on the solution composition.

2. Experimental

The experimental arrangement regarding the electrolysis cell, the electrodes and their preparation, the chemicals employed and the solution preparation, were as already reported in previous publications [10]. Specpure nickel electrodes were used (area = 0·25 cm^2).

The following solutions were used: 1 M KOH (Solution 1), 0·1 M KOH + 0·6 M K_2SO_4 (Solution 2); 0·01 M KOH + 0·66 M K_2SO_4 (Solution 3); and 0·1 M KOH (Solution 4). Runs were made at 25° C under 1 atm pressure of nitrogen and the nickel working electrode was referred to the NHE scale. The Ni/alkaline solution interfaces were perturbed with a triangularly-modulated repetitive triangular potential sweep (TMTPS) with the following characteristics: base signal sweep rate, $0{\cdot}1 \leqslant v_b \leqslant 2\ V\ s^{-1}$; base signal switching potentials, $0{\cdot}6 \leqslant E^b_{\lambda,a} \leqslant 0{\cdot}9$ V and $0{\cdot}2 \leqslant E^b_{\lambda,c} \leqslant 0{\cdot}4$ V; modulating signal sweep rate, $2 \leqslant v_m \leqslant 50\ V\ s^{-1}$; modulating signal amplitudes, $0{\cdot}03 \leqslant \Delta E^m \leqslant 0{\cdot}15$ V. The complex E/I displays were photographed from the 502 A Tektronix oscilloscope screen.

3. Results

When an electrochemical reaction involves the formation of thin layers of active materials on the electrode surface the corresponding electrochemical characteristics are more directly interpreted after comparing the conventional E/I displays run under a repetitive triangular potential sweep (RTPS) with those obtained under a TMTPS (Fig. 1). The E/I trace resulting from the TMTPS

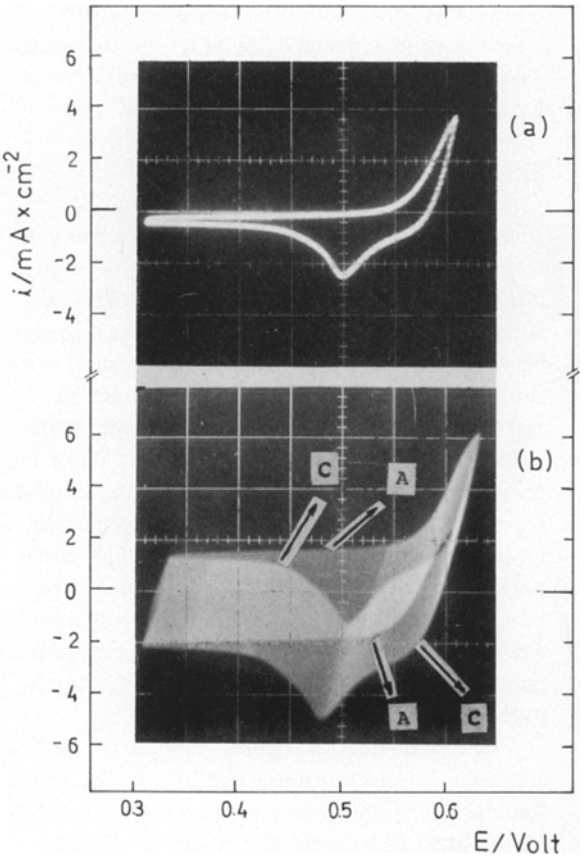

Fig. 1. Comparison between RTPS and TMTPS voltammograms run between $E_{\lambda,c} = 0{\cdot}31$ V and $E_{\lambda,a} = 0{\cdot}62$ V: (a) $v = 0{\cdot}2\ V\ s^{-1}$; (b) $v_b = 0{\cdot}2\ V\ s^{-1}$; $v_m = 20\ V\ s^{-1}$, $\Delta E_m = 0{\cdot}03$ V. Solution 1.

perturbation is certainly much more complex than the conventional TPS E/I display. The displays shown in Fig. 1 establish the basis for the interpretation of the data and contain practically the same kinetic information because of the choice of perturbation conditions used. They exhibit a double contour for both the anodic (A) and the cathodic scans (C) which in the simplest cases resemble the E/I profiles recorded under TPS perturbations. The TMTPS E/I profile, however, presents a fine structure covering the gap of each pair of contours due to the modulating frequency. The gap itself involves also the current jump produced by the charging and discharging of the DL capacitance. The current jump is produced each time the slope of the modulating signal changes sign. The E/I contour recorded during the anodic scan involves different anodic and cathodic current contributions from those pertaining to the cathodic scan (the anodic and cathodic currents are referred to the $I = 0$ baseline). Moreover, the fine structure gives direct information about the corresponding conjugated redox couples playing a part during the perturbation process and their degree of reversibility. For a rapid process, the ideal response of the system would correspond to a vertical current jump between the envelopes, while an increasing irreversibility should produce a progressively steeper E/I response for each modulating cycle. Under the perturbation conditions used for Figs. 1a and b, the overall anodic charge equals the overall cathodic charge. The charge excess observed in the TMTPS is due to the electrical double-layer capacitance, whose contribution is magnified by the magnitude of the potential sweep rate of the modulating signal.

For the case of the Ni–Solution 1 interface under the set of perturbation conditions indicated in Fig. 2, the TMTPS E/I display exhibits the following outstanding characteristics. During the anodic scan, at about 0·55 V there is a net increase of the anodic current and simultaneously a clear definition of a cathodic current peak at about 0·54 V. At a higher anodic potential another redox system is formed, with an anodic current peak at 0·63 V while the corresponding cathodic

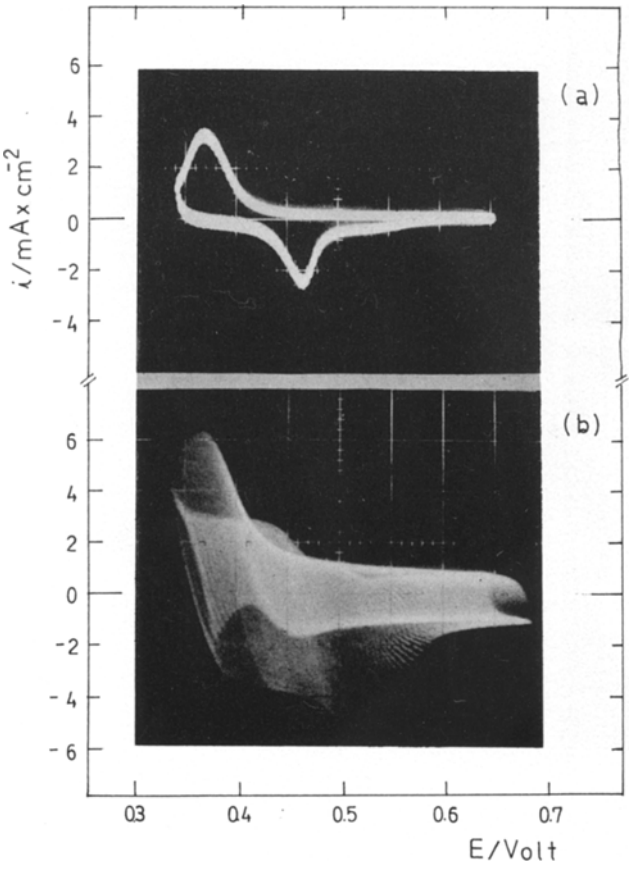

Fig. 2. Comparison between RTPS and TMTPS voltammograms run between $E_{\lambda,c} = 0{\cdot}33$ V and $E_{\lambda,a} = 0{\cdot}66$ V: (a) $v = 0{\cdot}2\ \mathrm{V\,s^{-1}}$; (b) $v_b = 0{\cdot}2\ \mathrm{V\,s^{-1}}$; $v_m = 5\ \mathrm{V\,s^{-1}}$, $\Delta E_m = 0{\cdot}06$ V. Solution 1.

current peak, although it exists, is not very well distinguished because it lies just in the potential range which interferes with the returning excursion. Unfortunately the anodic switching potential is limited by the oxygen discharge reaction.

During the cathodic excursion there is an appreciable current contribution in the range 0·65–0·55 V approximately. In the region of 0·55 V both currents just exceed the currents recorded at the same potential during the anodic excursion. At more cathodic potentials the cathodic current is much larger, a clear cathodic current peak is defined at 0·48 V plus a shoulder at about 0·45 V. During the cathodic excursion the fine structure of the *E/I* display shows an increasing irreversibility as the potential sweep reaches the cathodic switching potential, namely in the 0·50 V–0·41 V range. These *E/I* displays reveal, therefore, that three electrochemical systems are involved under these conditions in the nickel hydroxide electrode potential range.

The most clear description of the three electrochemical systems is obtained under the conditions shown in Fig. 3. Under these circumstances the cathodic potential excursions show the occurrence of an anodic current peak at 0·53 V which is complementary to the cathodic shoulder at about 0·50 V. The fine structure confirms the existence of a conjugated redox system whose definition depends to a large extent on the amplitude of the modulating frequency as well as on $E^{b}_{\lambda,a}$ and $E^{b}_{\lambda,c}$.

The characteristics of the *E/I* profiles just described are in principle the same for the other Ni–solution interfaces, except that the charge distribution of the different current peaks favours the

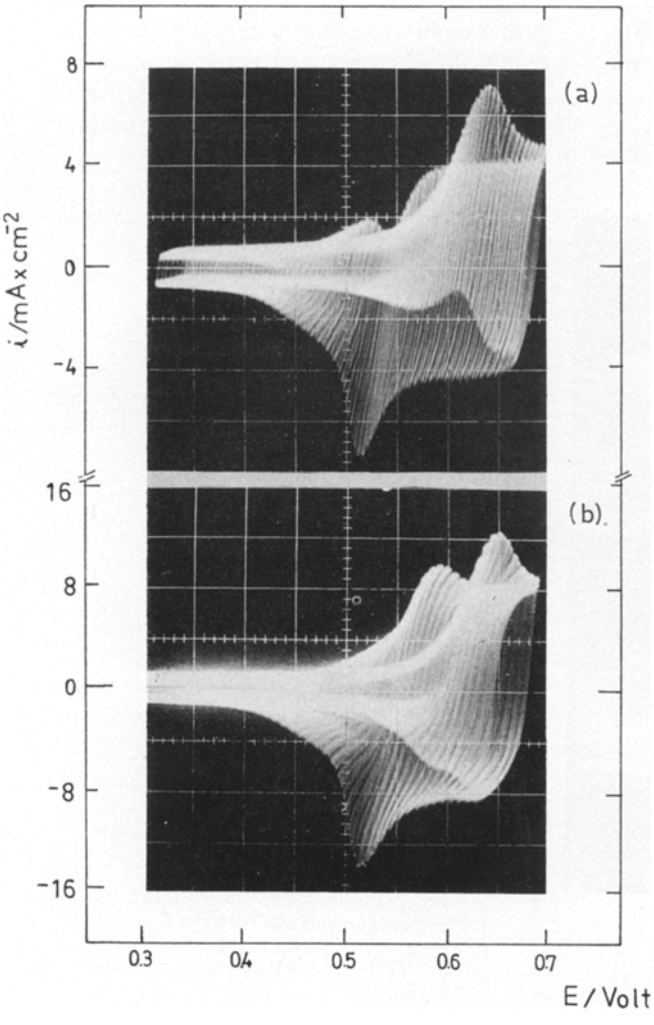

Fig. 3. *E/I* profiles run with TMTPS. (a) $v_b = 0{\cdot}2\ V\ s^{-1}$, $v_m = 5\ V\ s^{-1}$, $\Delta E_m = 0{\cdot}03$ V. (b) $v_b = 0{\cdot}2\ V\ s^{-1}$, $v_m = 8\ V\ s^{-1}$, $\Delta E_m = 0{\cdot}06$ V. Solution 1.

more stable reaction products during the cathodic excursion (Fig. 4) for the Ni–Solution 3 interface. This effect is also observed with the Ni–Solution 2 interface.

The potential difference between the anodic current peak potentials is 0·05 ± 0·01 V in good coincidence with the previously reported data obtained from linear potential sweep measurements [3]. The corresponding current peaks located at 0·65 V and 0·60 V were assigned to the electro-oxidation of the β-$Ni(OH)_2$ and α-$Ni(OH)_2$, respectively.

4. Discussion

The characteristics for the nickel hydroxide electrode under the above perturbation conditions confirm the equality of the total anodic and cathodic charges and show conclusively the complex nature of the reaction.

Previous studies [1, 2] made in 1 M KOH indicate that the kinetics of the overall process

$$Ni(OH)_2 = NiOOH + H^+ + e \qquad (2)$$

can be interpreted in terms of the square reaction Scheme 1. By holding the charge balance the proposed model explains to a large extent the ageing effects of either reactants or products.

The present results, however, show that under certain circumstances other intermediate species are participating in the overall reaction. Actually three conjugate redox couples play a part in the electrochemical reaction under non-equilibrium conditions. Their occurrence is related to topochemical changes of the surface species. The existence of these reactions was recently predicted [3].

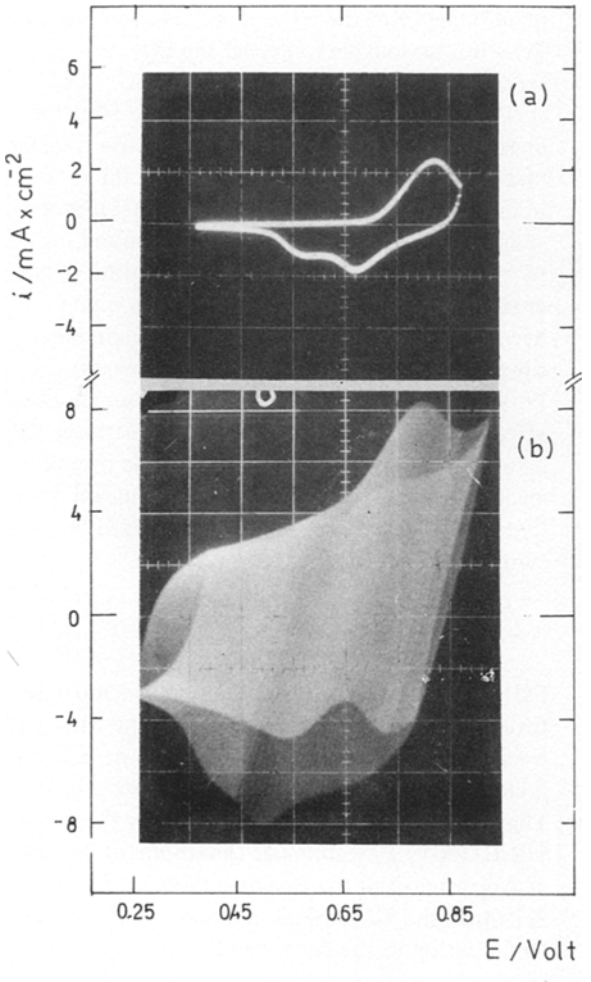

Fig. 4. Comparison between RTPS and TMTPS voltammograms in Solution 3. (a) $v_b = 0{\cdot}2\ V\,s^{-1}$; (b) $v_b = 0{\cdot}2\ V\,s^{-1}$, $v_m = 20\ V\,s^{-1}$, $\Delta E_m = 0{\cdot}15$ V.

The electrochemical reactions pertaining to these new species are more clearly detected when the SO_4^{2-}/OH^- concentration ratio increases. Under these circumstances a new $Ni(OH)_2$-type species more labile than α-$Ni(OH)_2$ apparently exists. It is electro-oxidized to the more unstable NiOOH species without being able to undergo transformation into either the α- or the β-$Ni(OH)_2$ species. The corresponding redox system should be responsible for the appearance of the current peaks in the envelopes of the TMTPS. Consequently the Reaction Scheme 1 can be put forward in the following more extended form

$$\begin{array}{ccc} [Ni(OH)_2]_u & \overset{(i)}{\rightleftharpoons} & [NiOOH]_s + H^+ + e \\ \downarrow (iv) \quad \searrow & & \nearrow \quad \uparrow (iii) \\ & [Ni(OH)_2]^* & \\ \swarrow \quad \downarrow & & \nearrow \quad \rightleftharpoons \\ [Ni(OH)_2]_s & \overset{(ii)}{\rightleftharpoons} & [NiOOH]_u + H^+ + e \end{array} \qquad (3)$$

where $[Ni(OH)_2]^*$, represents the simplest stoichiometry for the compound bridging both main electrochemical and chemical processes participating in the square reaction model. The dashed arrows refer to possible reactions which are not detected under the present experimental conditions. The subscripts s and u refer to stable and unstable species, respectively.

The influence of the potential sweep rate and amplitude of the modulating signal on the distribution of the current peaks during the cathodic scan may be noted. With a fast potential sweep and small amplitude of the modulating signal, Reactions (i) and (ii) in Scheme 3 behave as simple reversible electrochemical reactions since the surface concentration distribution of the NiOOH species anodically formed remains practically unchanged because of the relatively low value of the apparent rate constants of Reactions (iii) and (iv) [2]. On the contrary, with a slow potential sweep the contribution of Reaction (iii) becomes appreciable so that during the cathodic scan the electrochemical step (i) in the reverse direction becomes more important than during the anodic scan. Moreover, the contribution of Reaction (i) during the anodic excursion depends upon the distribution of the $Ni(OH)_2$ species attained when the cathodic switching potential is reached. This explains the kind of limiting anodic and cathodic currents which are observed during the triangularly-modulated cathodic potential scan in the 0·55–0·65 V range, under a certain set of perturbation conditions.

The currents related to the conjugated redox couple represented by Reaction (v) are located at about 0·53 V (anodic current peak) and at about 0·45 V (cathodic half-wave potential). The contribution of this reaction becomes significant as the SO_4^{2-}/OH^- concentration ratio increases. For the 1 M KOH solution its participation in the overall process is low, justifying the square reaction sequence (Scheme 1). If the contribution of Reaction (v) is appreciable one would expect the anodic and cathodic current peak half-widths in the nickel hydroxide potential range to increase as the SO_4^{2-}/OH^- concentration ratio increases. This effect has been recently reported [2].

A possible explanation for the stabilization of the $[Ni(OH)_2]^*$-type species can be given in terms of the competitive adsorption between SO_4^{2-} and OH^- ions. On the anodic side of the potential of zero charge of the Ni–alkaline solution interface [11] it is reasonable to expect the SO_4^{2-} ion specific adsorption to increase as the SO_4^{2-}/OH^- concentration ratio increases. Since the SO_4^{2-} ion does not participate in any direct electron transfer reactions within the potential range of the nickel hydroxide electrode, it probably interferes in the stabilization of the intermediate compound formed by the cathodic reaction. The contribution of the crossed reactions in the square reaction model becomes, therefore, increasingly important when the SO_4^{2-}/OH^- concentration ratio increases. Probably the competitive adsorption process also affects the rate of the topochemical reactions. The actual influence of the SO_4^{2-} ions on the overall electrochemical process related to the nickel hydroxide electrode can now be envisaged in terms of the processes described above.

Acknowledgement

INIFTA is sponsored by the Consejo Nacional de Investigaciones Científica y Técnicas, the Universidad Nacional de La Plata and the Comisión de Investigaciones Científicas (Provincia de Buenos Aires). This work is also partially sponsored by the SENID (Navy Research and Development Service of Argentina) and the Regional Program for the Scientific and Technological Development of the Organization of the American States.

References

[1] J. R. Vilche and A. J. Arvia, *4th International Symposium on Passivity*, Virginia (1977).

[2] R. S. Schrebler Guzmán, J. R. Vilche and A. J. Arvia, *J. Appl. Electrochem.* 8 (1978) 67.

[3] R. S. Schrebler Guzmán, J. R. Vilche and A. J. Arvia, *J. Electrochem. Soc.* in press.

[4] H. Bode, K. Dehmelt and J. Witte, *Z. Anorg. Chem.* 366 (1969) 1.

[5] D. M. MacArthur, *J. Electrochem. Soc.* 117 (1970) 422.

[6] G. W. D. Briggs, 'Electrochemistry' Vol. 4, p. 33, Specialist Periodical Reports, The Chemical Society, London (1974).

[7] B. E. Conway and S. Gottesfeld, *J. Chem. Soc. Faraday Trans. I.* 69 (1973) 1090.

[8] N. R. de Tacconi, J. O. Zerbino and A. J. Arvia, *J. Electroanalyt. Chem.* 79 (1977) 287.

[9] C. M. Ferro, A. J. Calandra and A. J. Arvia, *ibid* 53 (1974) 231.

[10] J. R. Vilche and A. J. Arvia, *Corros. Sci.* 15 (1975) 419.

[11] J. O'M. Bockris, S. D. Argade and E. Gileadi, *Electrochim. Acta* 14 (1969) 1267.